HHS Public Access

Author manuscript

Mol Imaging Biol. Author manuscript; available in PMC 2017 December 01.

Published in final edited form as:

Mol Imaging Biol. 2017 October ; 19(5): 754–761. doi:10.1007/s11307-017-1049-y.

Development of a New Folate-Derived Ga-68-Based PET Imaging Agent

Christian Brand[1], **Valerie A. Longo**[2], **Mike Groaning**[3], **Wolfgang A. Weber**[1,4,5], and **Thomas Reiner**[1,5]

[1]Department of Radiology, Memorial Sloan Kettering Cancer Center, 1275 York Avenue, New York, NY, 10065, USA

[2]Small-Animal Imaging Core Facility, Memorial Sloan Kettering Cancer Center, New York, NY, 10065, USA

[3]Endocyte, Inc., West Lafayette, IN, 47906, USA

[4]Molecular Pharmacology and Chemistry Program, Memorial Sloan Kettering Cancer Center, New York, NY, 10065, USA

[5]Weill Cornell Medical College, Cornell University, New York, NY, 10065, USA

Abstract

Purpose—The folate receptor (FR) has emerged as an interesting diagnostic and therapeutic drug target with many potential applications in oncologic and inflammatory disorders. It was therefore the aim of this study to develop a folate-derived Ga-68-based positron emission tomography (PET) imaging tracer that is straightforward to radiolabel and could be broadly used in clinical studies. We validated its target binding affinity and specificity and compared it to [^{99m}Tc]EC20, the folate single-photon emission computed tomography (SPECT) imaging tracer that has been most extensively studied clinically so far.

Procedures—The new folic acid-derived PET imaging agent is linked via a polyethyleneglycol linker to the chelator 1,4,7-triazacyclononane-1,4,7-trisacetic acid (NOTA). This new compound, NOTA-folate, was labeled with gallium-68. We tested the probe's stability in human plasma and its selectivity *in vitro*, using the FR-positive KB cell line as well as the FR-negative A549 cell line. The pharmacokinetic profile of [^{68}Ga]NOTA-folate was evaluated in FR-positive KB mouse xenografts. Following intravenous injection of [^{68}Ga]NOTA-folate (383 ± 53 μCi), PET/computed tomography (CT) imaging studies as well as biodistribution studies were performed using KB tumor-bearing mice (n = 3). *In vitro* as well as *in vivo* studies were performed in parallel with the SPECT imaging tracer [^{99m}Tc]EC20.

Correspondence to: Wolfgang Weber; weberw@mskcc.org, Thomas Reiner; reinert@mskcc.org.

Electronic supplementary material The online version of this article (doi:10.1007/s11307-017-1049-y) contains supplementary material, which is available to authorized users.

Compliance with Ethical Standards

Conflict of Interests

M.G. is an employee of Endocyte, Inc.

Results—In comparison to [^{99m}Tc]EC20 (radiochemical yield (RCY) = 82.0 ± 2.9 %, 91.8 ± 2.0 % purity), similar radiochemical yield (87.2 ± 6.9 %) and radiochemical purity (95.6 ± 1.8 %) could be achieved for [^{68}Ga]NOTA-folate. For both tracers, we observed high affinity for FR-positive cells *in vitro* and high plasma stability. In PET/CT and biodistribution studies, [^{68}Ga]NOTA-folate appeared to display slightly superior *in vivo* performance in comparison to [^{99m}Tc]EC20. In detail, ^{68}Ga-NOTA-folate showed very good tumor uptake and retention (6.6 ± 1.1 %ID/g), relatively low kidney uptake (21.7 ± 1.1 %ID/g), and very low liver uptake (0.38 ± 0.08 %ID/g). *In vivo* blocking studies using a fivefold excess of EC20 reduced the tumor uptake to 2.5 ± 0.7 %ID/g, confirming receptor specific binding of [^{68}Ga]NOTA-folate *in vivo*.

Conclusion—We validated a new Ga-68 folate-based PET imaging agent with excellent pharmacokinetics and tumor uptake. Based on a head-to-head comparison between both tracers, [^{68}Ga]NOTA-folate is a suitable imaging probe for the delineation of FR-positive tumors and a promising candidate for clinical translation.

Keywords

PET imaging; Folate receptor expression; Small molecule; SPECT

Introduction

The folate receptor (FR) has emerged as a valuable target for treating a range of cancers, and several targeted therapies directed toward folate receptors are in late-stage clinical development [1, 2]. These therapies build on the high affinity of folic acid and its derivatives to folate receptors (K_D(folate) = 0.1 nM) [3, 4], paired with the receptor's overexpression in a wide variety of human epithelial cancers [5–8]. In parallel to the development of FR-targeted therapeutics, radio and optical tracers have been developed, and folate receptor-targeted imaging has been used successfully in preclinical and clinical research [8–14]. Similar to what is observed for folic acid, conjugates bearing these agents are bound to the folate receptor, and they are transported into the cell by endocytosis [15]. Preclinical and clinical studies also revealed uptake of folate-targeted imaging agents in areas of inflammatory diseases such as rheumatoid arthritis and could be connected to folate receptor expression on activated macrophages [16, 17].

Clinical studies of folate-targeting drugs would benefit enormously from a method to quantify FR expression levels in whole-body studies as there is well-known inter- and intra-patient variability in FR expression levels in patients with metastatic cancers [18, 19]. The single-photon emission computed tomography (SPECT) imaging agent [^{99m}Tc]EC20 was used in several clinical trials as a companion imaging agent for small molecular folate therapeutics. However, a positron emission tomography (PET) imaging agent would have significant advantages, including a faster image acquisition as well as a more robust quantification of the concentration of FR ligands in tumor and normal organs [20].

With this in mind, we became interested in designing, testing, and validating a folate-targeted probe that allows imaging and easy quantification of folate receptors. Our goal was to validate a small-molecule folate PET agent that (1) quickly distributes throughout tissue, (2) targets folate receptors with high affinity, (3) efficiently clears from non-targeted sites

and compartments, and (4) demonstrates high tumor uptake for sensitive detection of FR expression even in small lesions. We not only report the development and preclinical evaluation of this new agent, [^{68}Ga]NOTA-folate, but we also compare its *in vitro* and *in vivo* performance to the already clinically used SPECT tracer [^{99m}Tc]EC20.

Materials and Methods

Materials

Unless otherwise stated, all chemicals and solvents were used without further purification. Water used for this study was ultrapure (>18.2 MΩ cm^{-1} at 25 °C), and acetonitrile (CH_3CN) as well as ethanol were of HPLC grade purity. Chelexed water was prepared with BT Chelex 100 Resin (Bio-Rad) and phosphate-buffered saline (PBS) was purchased from the media preparation facility at Memorial Sloan Kettering Cancer Center. Ascorbic acid and sodium hydroxide were purchased from Sigma-Aldrich as TraceSELECT (>99.9 % purity). All other chemicals were acquired from Sigma-Aldrich unless stated otherwise. Waters Sep-Pak C18 Plus Light cartridges were purchased from Fisher Scientific (Pittsburgh, PA). The precursor for PET imaging, NOTA-folate, as well as the labeling kit for radiolabeling EC20 were provided by Endocyte (West Lafayette, IN). Ga-68 was produced by a Ge-68/Ga-68 generator from ANSTO (Sydney, Australia). Sodium [^{99m}Tc]pertechnate was supplied by Nuclear Diagnostic Product (Rockaway, NJ). The human epithelial cancer cell line KB as well as the human lung cancer cell line A549 were purchased from ATCC (Manassas, VA) and grown by serial passage. All HPLC purifications and quality controls (0.5 ml/min, buffer A = 0.1 % TFA in water, buffer B = 0.1 % TFA in acetonitrile) were performed on a Shimadzu UFLC HPLC system equipped with a DGU-20A degasser, SPD-M20A UV detector, LC-20AB pump system, CBM-20A communication BUS module, and a Scan-RAM radio-TLC/HPLC-detector form Lablogic using a reversed phase Phenomenex Luna column (2.5 μm, C-18(2)-HST, 50 × 3.0 mm). Liquid chromatography-mass spectrometry (LC-MS) was recorded with an LCMS-2020 Shimadzu system.

Preparation of [^{99m}Tc]EC20

The preparation of the SPECT imaging tracer [^{99m}Tc]EC20 was performed according to Leamon et al. [21] using an EC20 labeling kit, containing a lyophilized mixture of EC20 (0.1 mg, 0.13 μmol, 745.2 g/mol); sodium α-D-glucoheptonate (80.0 mg, 0.32 mmol, 248.2 g/mol); tin(II)chloride dihydrate (80.0 mg, 0.35 mmol); and sufficient sodium hydroxide or hydrochloric acid to adjust the pH to 6.8 (prior to lyophilization). Chelexed water (1.0 ml) was added to the vial of the radiolabeling kit. Thereafter, 224 μl of the EC20 solution (22.4 μg, 30.1 nmol) was added to a solution of sodium [^{99m}Tc]pertechnate (13.9 ± 1.4 mCi, 514 ± 52 MBq, 0.15 ml), and the reaction solution was placed on a thermomixer and agitated at 600 rpm for 30 min at 80 °C. After cooling to room temperature, the product was purified using a Sep-Pak C18 light cartridge as previously described [21]. The solution of [^{99m}Tc]EC20 (11.4 ± 0.65 mCi, 422 ± 24 MBq (decay-corrected), radiochemical yield (RCY) = 82.0 ± 2.9 %) in ethanol/PBS (1:1, 400 μl) with a specific activity of 0.38 ± 0.02 Ci/μmol (14.0 ± 0.07 GBq/μmol) was further diluted with PBS (1.6 ml) and used for *in vitro* as well as *in vivo* studies ~60 min post synthesis.

Preparation of [^{68}Ga]NOTA-Folate

NOTA-folate (Fig. 1) was provided by Endocyte (West Lafayette, IN). The small molecule was obtained in ≥97 % chemical purity, as confirmed by RP-HPLC at 254 nm (Fig. S1a). Observed masses in liquid chromatography-mass spectrometry (LC-MS) were 857.2 $[M+H]^+$ and 429.3 $[M+2H]^{2+}$ for NOTA-folate, with a theoretical mass of 856.38 g/mol (Fig. S1a, b).

For radiolabeling, a solution of NOTA-folate (25.8 μL, 25.8 μg, 30.1 nmol) in water was added to a solution of ascorbic acid (1 M, 200 μl) and NH_4OAc buffer (1 M, 500 μl). Then, $[^{68}Ga]GaCl_3$ in 0.3 M HCl (9.3 ± 1.6 mCi, 344 ± 59 MBq) was added to the reaction mixture (pH = 5.3), and the solution was placed on a thermomixer and agitated at 600 rpm for 15 min at 40 °C. After incubation, the [^{68}Ga]NOTA-folate was purified using pre-conditioned SEP-PAK C18 light cartridges to yield the completed radioligand (8.1 ± 1.8 mCi, 300 ± 67 MBq (decay-corrected), RCY = 87.2 ± 6.9 %) in >95 % radiochemical purity in a solution of ethanol/PBS (1:1, 400 μl) with a specific activity of 0.27 ± 0.06 Ci/μmol (9.97 ± 2.22 GBq/μmol). Then, the radioligand was further diluted with PBS (1.6 ml) and used for *in vitro* as well as *in vivo* studies ~60-min post synthesis.

Cell Culture

The human epithelial cancer cell line KB, a folate receptor-positive cell line, and the human cell line A549, a folate receptor-negative lung cancer cell line, were used for *in vitro* receptor binding studies at passages 3–11. Cell culture was performed as previously described [22]. KB cells were grown in folate-free RPMI 1640 medium (10 % FBS) from Gibco (ThermoFisher) containing L-glutamine (2.0 mM) and sodium bicarbonate buffer (2.0 g/L) and passaged regularly at 70–80 % confluence every 4–5 days. A549 cells were grown in RPMI 1640 medium (10 % FBS) from the media preparation facility at Memorial Sloan Kettering Cancer Center (New York, NY, USA) containing L-glutamine (2.0 mM) and sodium bicarbonate buffer (2.0 g/L) and passaged regularly at 70–80 % confluence every 3–4 days.

In Vitro Receptor Uptake Assay

Twenty-four hours prior to the *in vitro* studies, KB cells as well as A549 cells (1.0×10^6 cells/well, >90 % viability for both lines) were seeded into 6-well plates containing folate-free RPMI 1640 medium (2.0 ml) and incubated to form subconfluent monolayers of the cells. Then, medium was removed from the wells, cells were washed with PBS (1 ml) and medium (900 μl) was added. After 30 min of incubation at 37 °C, the radiotracer (0.1 nmol, 100 μl) in PBS was added to the dedicated well (c = 100 nM). For blocking studies, cells were pre-incubated with an excess of folate (c = 10 μM) 5 min prior to the addition of radiotracer. After 30 min post incubation at 37 °C, the supernatant of each well was collected together with washing solution (ice-cold PBS, 2 × 1.0 ml). Then, cells were treated with 1 M sodium hydroxide solution (1.0 ml) for 10 min at room temperature. Finally, cell suspension was collected together with washing solution (ice-cold PBS, 2 × 1.0 ml). The radioactivity of all contents including initially added radiotracer (0.1 nmol, 100 μl) was measured using a WIZARD^2 automatic γ-counter from PerkinElmer. Receptor-specific

uptake was calculated by cell-bound activity and expressed as a percentage of applied activity per million cells.

Serum Protein Binding

The radiotracers (1.8 ± 0.5 mCi, 67 ± 19 MBq, 360 μl) were incubated while agitated (600 rpm) at 37 °C in human serum (1.0 ml, Sigma-Aldrich). At pre-determined time points (30, 60, 120, and 240 min), 250 μl of the serum was transferred in to a 1.7-ml Eppendorf tube containing ice-cold acetonitrile (250 μl). The resulting mixture was vortexed (1 min) and centrifuged (13,000 rpm) for 5 min. The supernatant was transferred into a 1.7-ml Eppendorf tube followed by additional centrifugation at 13,000 rpm for 2 min. Afterwards, the supernatant was diluted with water (150 μl), radioactivity was measured, and the resulting solution was used for HPLC analysis. The residual pellet of protein was checked for radioactivity to determine serum protein binding of the radiotracer as well.

Animals

All mouse model experiments and procedures were performed in accordance to an approved protocol from the Institutional Animal Care and Use Committee at Memorial Sloan Kettering Cancer Center. Prior to small-animal imaging studies, female athymic nude mice (Charles River; outbred; 6–8 weeks, 20–25 g) were subjected to a specific low-folate diet (AIN-93G/0.0 ppm folate one half IRR) from TestDiet (St. Louis, MO) for 2 weeks. Then, suspended KB cells (1.5×10^6, viability: >93 %) in a 1:1 mixture of media/matrigel (150 μl) were subcutaneously inoculated into the right shoulder of anesthetized mice (2 % isoflurane gas in 2 l/min medical air) to establish tumors (100–150 mm^3) after 7–9 days. For intravenous injections, mice were gently heated with a heating lamp placed on an injection restrainer, tail cleaned with sterilized alcohol pads, and the imaging agent was injected into the lateral tail vain. On average, there was about 60-min delay between the end of the synthesis and administration to the animals.

PET/CT Imaging

PET scans were performed using a small-animal Inveon® PET/CT system from Siemens (Knoxville, TN). [^{68}Ga]NOTA-folate (383 ± 53 μCi, 14.2 ± 2.0 MBq, 3.1 nmol, 200 μl PBS containing 10 % ethanol) alone or a mixture of [^{68}Ga]NOTA-folate (222 ± 25 μCi, 8.2 ± 0.9 MBq, 3.1 nmol, 200 μl PBS containing 10 % ethanol) and EC20 (12.5 nmol) was injected into KB tumor-bearing female athymic nude mice ($n = 3$) vial tail vain. At 1, 2, and 4 h after injection, the mice were anesthetized with 1.5–2.0 % isoflurane (Baxter Healthcare) at 2 ml/min in oxygen and PET/CT imaging was accomplished over 15 min. Images were analyzed using AsiPro VM™ software (Concorde Microsystems) and Inveon research workplace 4.1 software (Siemens Healthcare).

SPECT/CT Imaging

SPECT/CT scans were performed using a small-animal NanoSPECT/CT from Mediso Medical Imaging Systems (Boston, MA). [^{99m}Tc]EC20 (501 ± 11 μCi, 18.5 ± 0.4 MBq, 3.1 nmol, 200 μl PBS containing 10 % ethanol) was administered into KB tumor-bearing female athymic nude mice ($n = 3$) via tail vein 24 h after PET studies. At 2 and 4 h post injection,

the mice were anesthetized with 1.5–2.0 % isoflurane (Baxter Healthcare) at 2 ml/min in oxygen and SPECT/CT data was collected over 30 min.

Biodistribution Experiments

Female athymic nude mice ($n = 3$) bearing subcutaneous KB (right shoulder) xenografts were euthanized after imaging studies (4 h post injection) through asphyxiation with CO_2. Organs of interested were harvested, weighed, and counted using a WIZARD^2 automatic γ-counter from PerkinElmer. The percentage of tracer uptake stated as percentage injected dose per gram of tissue (%ID/g) was calculated as the activity associated with tissue per organ weight per actual injected dose, decay-corrected to the start time of counting.

Statistical Analysis

Statistical analysis was performed by Prism software (version 6, GraphPad Software Inc.). The reported values are mean ± standard deviation.

Results

In Vitro Receptor Binding Studies

Figures 1 and 2 show the structures, key parameters and analytical data of [^{68}Ga]NOTA-folate and [^{99m}Tc]EC20. [^{68}Ga]NOTA-folate had cell-associated uptake values of around 2.84 ± 0.02 % per million cells compared to [^{99m}Tc]EC20 with 3.92 ± 0.22 % uptake per million cells (Fig. 3a and Fig. S5). Blocking experiments performed with an excess of folic acid showed less than 0.1 % nonspecific binding of both radiotracers, demonstrating their high specificity for the folate receptor *in vitro*. In addition, both radiotracers showed negligible uptake (0.28 ± 0.07 and 0.20 ± 0.07 % for [^{68}Ga]NOTA-folate and [^{99m}Tc]EC20) after 30 min of incubation at 37 °C with the FR-negative cell line A549.

Serum Stability and Protein Binding

Prior to *in vivo* tissue distribution studies, the *in vitro* stabilities of both imaging tracers, [^{99m}Tc]EC20 and [^{68}Ga]NOTA-folate, were determined by incubation of each imaging tracer with human plasma serum over a period of 240 min (Fig. 3b). In general, high relative stability (>95 %) of both radioligands could be observed over the 240-min time period. We also compared the protein binding of both tracers 30 min after incubation (Figure S4). [^{99m}Tc]EC20 binds to serum proteins to an extent of ~33 % after 30 min, whereas [^{68}Ga]NOTA-folate binds to serum protein at a lower extent of ~14 %.

PET/CT and SPECT Imaging Studies

Already after 1 h post injection, the PET images with [^{68}Ga]NOTA-folate showed high focal uptake in the tumor (5.66 ± 1.33 %ID/g) as well as activity in kidneys and bladder. There was also mild uptake in the GI tract. Neither for [^{68}Ga]NOTA-folate nor [^{99m}Tc]EC20, uptake in the salivary glands was observed [6]. Images at 2 and 4 h post injection showed no major change in the biodistribution (see Fig. S2). Tumor uptake at these two time points was 5.62 ± 1.46 and 5.67 ± 1.69 %ID/g, respectively. To show specificity of [^{68}Ga]NOTA-folate (252 μCi, 9.3 MBq, 3.1 nmol) toward folate receptor in whole-body PET imaging, we

further conducted blocking studies by co-injection of EC20 (12.5 nmol). PET demonstrated effective blocking of KB tumor uptake by NOTA-folate (Figs. 4 and 5).

The SPECT images with EC20 showed similar uptake of tumor, kidney, and bladder. In addition, tracer uptake was seen in the liver and gallbladder (Fig. S3).

Biodistribution Studies

The biodistribution results of [^{68}Ga]NOTA-folate and [^{99m}Tc]EC20 are presented in Fig. 4 and Table S1. The uptake (%ID/g) as well as the tumor-to-organ ratios of the imaging agents in selected organs of interest are summarized in Fig. 4. Tumor uptake of [^{99m}Tc]EC20 and [^{68}Ga]NOTA-folate were similar (7.88 ± 0.04 and 6.61 ± 1.07 %ID/g, $P = 0.477$ [unpaired student's t test]). The tumor uptake of [^{68}Ga]NOTA-folate was significantly reduced by co-injection of EC20 (2.57 ± 0.45 %ID/g, $P = 0.0284$ [unpaired student's t test]), indicating that tumor uptake of [^{68}Ga]NOTA-folate was due to folate receptor binding. [^{99m}Tc]EC20 also accumulated in folate receptor-expressing organs [21, 23, 24], first and foremost the kidneys (26.11 ± 0.62 %ID/g). [^{68}Ga]NOTA-folate, in comparison, showed slightly less uptake (21.65 ± 1.11 %ID/g; $P = 0.0497$) in the kidneys, but more importantly liver uptake of [^{68}Ga]NOTA-folate was sevenfold lower than that of [^{99m}Tc]EC20 (0.38 ± 0.08 vs. 2.48 ± 0.69 %ID/g; $P < 0.0088$, [unpaired student's t test]). Furthermore, blood activity levels were significantly lower for [^{68}Ga]NOTA-folate than for [^{99m}Tc]EC20 (0.07 ± 0.01 vs. 0.22 ± 0.05 %ID/g, $P = 0.0091$ [unpaired student's t test]) indicating faster blood clearance. In summary, the new PET imaging tracer showed a similar biodistribution and tumor uptake as [^{99m}Tc]EC20 with the important distinction of having markedly lower liver uptake.

Discussion

The results of this study indicate that [^{68}Ga]NOTA-folate could be a promising agent for imaging folate receptors with PET. [^{68}Ga]NOTA-folate was found to be straightforward to radiolabel and showed excellent stability and favorable biodistribution in tumor-bearing mice. These characteristics allowed for imaging of folate receptor-positive tumors with high contrast.

We compared [^{68}Ga]NOTA-folate with [^{99m}Tc]EC20, a folate receptor targeting imaging agent that has been tested in more than 13 clinical trials and has been administered to more than 1000 patients. In these studies, tumor uptake of [^{99m}Tc]EC20 has been shown to correlate with folate expression levels in various tumors. Based on these data, [^{99m}Tc]EC20 is currently investigated as a tool to select patients for treatment with folate receptor targeted small-molecule drug conjugates (SMDCs) such as vintafolide [25, 26]. A PET imaging agent with similar tumor uptake and pharmacokinetics as [^{99m}Tc]EC20 is likely to improve characterization of small lesions due to the higher spatial resolution of clinical PET and would enable robust quantitative assessment of radiotracer uptake by tumors and normal organs. Therefore, we performed a head-to-head comparison of [^{68}Ga]NOTA-folate with [^{99m}Tc]EC20 in this study.

Cellular uptake of [^{68}Ga]NOTA-folate in folate receptor-positive tumor cells was similar to [^{99m}Tc]EC20 and was almost completely blocked by incubation with an excess of unlabeled

EC20, confirming folate receptor specific uptake of [^{68}Ga]NOTA-folate. Human plasma stability studies revealed that both tracers, [^{68}Ga]NOTA-folate and [^{99m}Tc]EC20, have high *in vitro* stabilities (>95 %). However, [^{99m}Tc]EC20 has a higher plasma protein binding (32.5 ± 1.2 and 13.8 ± 0.4 % for [^{99m}Tc]EC20 and [^{68}Ga]NOTA-folate, respectively, $P <$ 0.0001, [unpaired student's *t* test], Fig. S4).

This discrepancy in protein binding may have contributed to the sevenfold lower liver uptake of ^{68}Ga-NOTA-folate as compared [^{99m}Tc]EC20 (0.38 ± 0.08 vs. 2.48 ± 0.69 %ID/g, $P <$ 0.0088, [unpaired student's *t* test], Fig. 4). In clinical studies, high hepatic uptake of [^{99m}Tc]EC20 is known to limit detection of liver metastases or hepatic implants—an important limitation for characterizing folate receptor status of ovarian cancer and other malignancies that frequently involve the liver. Therefore, the lower liver uptake (if confirmed in human studies) could be an advantage of [^{68}Ga]NOTA-folate. We also observed a faster blood clearance for [^{68}Ga]NOTA-folate than for [^{99m}Tc]EC20 and tumor uptake kinetics that very well fit the short physical half-life of Ga-68 (68 min).

High renal uptake is a characteristic of all folate receptor targeting imaging agents and is to a large extent a result of folate receptor expression by the proximal tubule cells of the kidney [27]. Therefore, it is expected that [^{68}Ga]NOTA-folate and [^{99m}Tc]EC20 show similar renal uptake. Both tumor-to-kidney (0.31 ± 0.11) and tumor-to-liver ratios (12.43 ± 0.73) seem comparable to other, previously published data for other folate-targeted radiopharmaceuticals [3, 14, 28–34]. For a direct comparison, however, the individual compounds would have to be tested side-by-side. There was no statistically significant difference between [^{68}Ga]NOTA-folate and [^{99m}Tc]EC20 uptake in KB tumors (6.61 ± 1.07 and 7.88 ± 0.04 %ID/g for [^{68}Ga]NOTA-folate and [^{99m}Tc]E20, respectively; $P <$ 0.48, [unpaired student's *t* test]). Surprisingly, uptake of the radiotracer in the saliva glands was not observed, in spite of their high folate expression [6].

As we have previously pointed out, the [^{68}Ga]NOTA-folate PET imaging agent is by far not the first folate-targeted PET conjugate described in the literature. As a matter of fact, numerous of folate-conjugated PET agents have already been proven to visualize FR-positive tumors *in vivo* [3, 28–31, 33–38]. In the past, different approaches were utilized for the synthesis of folate-based PET radiotracers. To our knowledge, current preclinical PET imaging tracers are based on either F-18 [14, 28–30, 33, 38] or Ga-68 [3, 31, 34–37] as a radionuclide for *in vivo* imaging. All imaging tracers were able to successfully delineate folate receptor-positive tumors in animal models. These previous results encouraged us explore additional folate-targeted PET imaging tracers that could potentially meet the requirements for translation into the clinic. Ga-68 was picked out ahead of F-18 not only because of its easier radiolabeling chemistry, but also because of the flexibility provided by long-lived Ge-68/Ga-68 generators that allow the synthesis of the radiotracer without an on-site cyclotron [3]. Here, we compared our folate-derived Ga-68-based PET imaging agent to [^{99m}Tc]EC20, a previously well-established imaging tracer, which was already used in several clinical trials for the delineation of folate receptor-positive solid tumors [39].

Conclusion

In summary, we radiolabeled and biologically characterized a new Ga-68 folate-targeted PET imaging agent. Excellent PET images of folate receptor-positive tumors were obtained in mice. In a head-to-head comparison with the established SPECT folate receptor imaging agent, [^{99m}Tc]EC20, the new ^{68}Ga-based imaging agent showed encouraging tumor to organ ratios *in vivo*. Thus, [^{68}Ga]NOTA-folate could be a suitable imaging probe to detect FR-positive tumors and to quantitatively assess their folate receptor expression levels.

Supplementary Material

Refer to Web version on PubMed Central for supplementary material.

Acknowledgments

The authors thank the Small Animal Imaging Core (P30 CA008748-48, S10 OD016207-01) and the Radiochemistry and Molecular Imaging Probes Core (P30 CA008748-48, S10 RR020892-01) for support. We also thank Endocyte, Inc. for generous support. The authors thank also Dr. Jason S. Lewis and Dr. NagaVaraKishore Pillarsetty for helpful discussions. Finally, the study was supported by grants from the National Institute of Health (K25 EB016673 for T.R.), the Center for Molecular Imaging and Nanotechnology of Memorial Sloan Kettering Cancer Center (for T.R.).

References

1. Vergote I, Leamon CP. Vintafolide: a novel targeted therapy for the treatment of folate receptor expressing tumors. Ther Adv Med Oncol. 2015; 7:206–218. [PubMed: 26136852]
2. Ab O, Whiteman KR, Bartle LM, et al. IMGN853, a folate receptor-α (FRα)-targeting antibody-drug conjugate, exhibits potent targeted antitumor activity against FRα-expressing tumors. Mol Cancer Ther. 2015; 14:1605–1613. [PubMed: 25904506]
3. Fani M, Tamma ML, Nicolas GP, et al. In vivo imaging of folate receptor positive tumor xenografts using novel ^{68}Ga-NODAGA-folate conjugates. Mol Pharm. 2012; 9:1136–1145. [PubMed: 22497506]
4. Kamen BA, Wang M-T, Streckfuss AJ, et al. Delivery of folates to the cytoplasm of MA104 cells is mediated by a surface membrane receptor that recycles. J Biol Chem. 1988; 263:13602–13609. [PubMed: 3417674]
5. Wu M, Gunning W, Ratnam M. Expression of folate receptor type a in relation to cell type malignancy, and differentiation in ovary, uterus, and cervix. Cancer Epidemiol Biomark Prev. 1999; 8:775–782.
6. Salazar MD, Ratnam M. The folate receptor: what does it promise in tissue-targeted therapeutics. Cancer Metastasis Rev. 2007; 26:141–152. [PubMed: 17333345]
7. Parker N, Turk MJ, Westrick E, et al. Folate receptor expression in carcinomas and normal tissues determined by a quantitative radioligand binding assay. Anal Biochem. 2005; 338:284–293. [PubMed: 15745749]
8. Low PS, Kularatne SA. Folate-targeted therapeutic and imaging agents for cancer. Curr Opin Chem Biol. 2009; 13:256–262. [PubMed: 19419901]
9. Müller C. Folate-based radiotracers for PET imaging—update and perspectives. Molecules. 2013; 18:5005–5031. [PubMed: 23629756]
10. Sega EI, Low PS. Tumor detection using folate receptor-targeted imaging agents. Cancer Metastasis Rev. 2008; 27:655–664. [PubMed: 18523731]
11. Leamon CP, Low PS. Folate-mediated targeting: from diagnostics to drug and gene delivery. Drug Discov Today. 2001; 6:44–51. [PubMed: 11165172]
12. Hilgenbrink AR, Low PS. Folate receptor-mediated drug targeting: from therapeutics to diagnostics. J Pharm Sci. 2005; 94:2135–2146. [PubMed: 16136558]

13. van Dam GM, Themelis G, Crane LM, et al. Intraoperative tumor-specific fluorescence imaging in ovarian cancer by folate receptor-α targeting: first in-human results. Nat Med. 2011; 17:1315–1319. [PubMed: 21926976]
14. Chen Q, Meng X, McQuade P, et al. Synthesis and preclinical evaluation of folate-NOTA-Al^{18}F for PET imaging of folate-receptor-positive tumors. Mol Pharm. 2016; 13:1520–1527. [PubMed: 27054811]
15. Leamon CP, Low PS. Delivery of macromolecules into living cells: a method that exploits folate receptor endocytosis. Proc Natl Acad Sci U S A. 1991; 88:5572–5576. [PubMed: 2062838]
16. Paulos CM, Turk MJ, Breur GJ, Low PS. Folate receptor-mediated targeting of therapeutic and imaging agents to activated macrophages in rheumatoid arthritis. Adv Drug Deliv Rev. 2004; 56:1205–1217. [PubMed: 15094216]
17. Low PS, Henne WA, Doorneweerd DD. Discovery and development of folic-acid-based receptor targeting for imaging and therapy of cancer and inflammatory diseases. Acc Chem Res. 2008; 41:120–129. [PubMed: 17655275]
18. O'Shannessy DJ, Somers EB, Maltzman J, et al. Folate receptor alpha (FRA) expression in breast cancer: identification of a new molecular subtype and association with triple negative disease. Springer Plus. 2012; 1:22. [PubMed: 23961352]
19. Stover PJ. Physiology of folate and vitamin B12 in health and disease. Nutr Res. 2004; 62:S3–S12.
20. Seo Y. Quantification of SPECT and PET for drug development. Curr Radiopharm. 2008; 1:17–21.
21. Leamon CP, Parker MA, Vlahov IR, et al. Synthesis and biological evaluation of EC20: a new folate-derived, Tc-based radiopharmaceutical. Bioconjug Chem. 2002; 13:1200–1210. [PubMed: 12440854]
22. Reddy JA, Westrick E, Santhapuram HK, et al. Folate receptor-specific antitumor activity of EC131, a folate-maytansinoid conjugate. Cancer Res. 2007; 67:6376–6382. [PubMed: 17616697]
23. Weitman SD, Lark RH, Coney LR, et al. Distribution of the folate receptor GP38 in normal and malignant cell lines and tissues. Cancer Res. 1992; 52:3396–3401. [PubMed: 1596899]
24. Ross JF, Chaudhuri PK, Ratnam M. Differential regulation of folate receptor isoforms in normal and malignant tissues in vivo and in established cell lines. Physiologic and Clinical Implications Cancer. 1994; 73:2432–2443. [PubMed: 7513252]
25. Morris RT, Joyrich RN, Naumann RW, et al. Phase II study of treatment of advanced ovarian cancer with folate-receptor-targeted therapeutic (vintafolide) and companion SPECT-based imaging agent (^{99m}Tc-etarfolatide). Ann Oncol. 2014; 25:852–858. [PubMed: 24667717]
26. Serpe L, Gallicchio M, Canaparo R, Dosio F. Targeted treatment of folate receptor-positive platinum-resistant ovarian cancer and companion diagnostics, with specific focus on vintafolide and etarfolatide. Pharmgenomics Pers Med. 2014; 7:31–42. [PubMed: 24516337]
27. Holm J, Hansen SI, Høier-Madsen M, Bostad L. A high-affinity folate binding protein in proximal tubule cells of human kidney. Kidney Int. 1992; 41:50–55. [PubMed: 1593862]
28. Al Jammaz I, Al-Otaibi B, Amer S, Okarvi SM. Rapid synthesis and in vitro and in vivo evaluation of folic acid derivatives labeled with fluorine-18 for PET imaging of folate receptor-positive tumors. Nucl Med Biol. 2011; 38:1019–1028. [PubMed: 21982573]
29. Bettio A, Honer M, Müller C, et al. Synthesis and preclinical evaluation of a folic acid derivative labeled with ^{18}F for PET imaging of folate receptor-positive tumors. J Nucl Med. 2006; 47:1153–1160. [PubMed: 16818950]
30. Boss SD, Betzel T, Müller C, et al. Comparative studies of three pairs of α- and γ-conjugated folic acid derivatives labeled with fluorine-18. Bioconjug Chem. 2016; 27:74–86. [PubMed: 26634288]
31. Fani M, Wang X, Nicolas G, et al. Development of new folate-based PET radiotracers: preclinical evaluation of ^{68}Ga-DOTA-folate conjugates. Eur J Nucl Med Mol Imaging. 2011; 38:108–119. [PubMed: 20799032]
32. Müller C, Forrer F, Schibli R, et al. SPECT study of folate receptor-positive malignant and normal tissues in mice using a novel ^{99m}Tc-radiofolate. J Nucl Med. 2008; 49:310–317. [PubMed: 18199624]
33. Ross TL, Honer M, Lam PY, et al. Fluorine-18 click radiosynthesis and preclinical evaluation of a new ^{18}F-labeled folic acid derivative. Bioconjug Chem. 2008; 19:2462–2470. [PubMed: 19053298]

34. Smith-Jones PM, Stolz B, Bruns C, et al. Gallium-67/gallium-68-[DFO]-octreotide—a potential radiopharmaceutical for PET imaging of somatostatin receptor-positive tumors: synthesis and radiolabeling in vitro and preliminary in vivo studies. J Nucl Med. 1994; 35:317–325. [PubMed: 8295005]

35. Mathias CJ, Lewis MR, Reichert DE, et al. Preparation of ^{66}Ga- and ^{68}Ga-labeled Ga(III)-deferoxamine-folate as potential folate-receptor-targeted PET radiopharmaceuticals. Nucl Med Biol. 2003; 30:725–731. [PubMed: 14499330]

36. Mathias CJ, Wang S, Lee RJ, et al. Tumor-selective radiopharmaceuticals targeting via receptor-mediated endocytosis of gallium-67-deferoxamine-folate. J Nucl Med. 1996; 37:1003–1008. [PubMed: 8683292]

37. Aljammaz I, Al-Otaibi B, Al-Hokbany N, et al. Development and pre-clinical evaluation of new ^{68}Ga-NOTA-folate conjugates for PET imaging of folate receptor-positive tumors. Anticancer Res. 2014; 34:6547–6556. [PubMed: 25368257]

38. Ross TL, Honer M, Müller C, et al. A new ^{18}F-labeled folic acid derivative with improved properties for the PET imaging of folate receptor-positive tumors. J Nucl Med. 2010; 51:1756–1762. [PubMed: 20956469]

39. Fisher RE, Siegel BA, Edell SL, et al. Exploratory study of ^{99m}Tc-EC20 imaging for identifying patients with folate receptor-positive solid tumors. J Nucl Med. 2008; 49:899–906. [PubMed: 18483093]

a

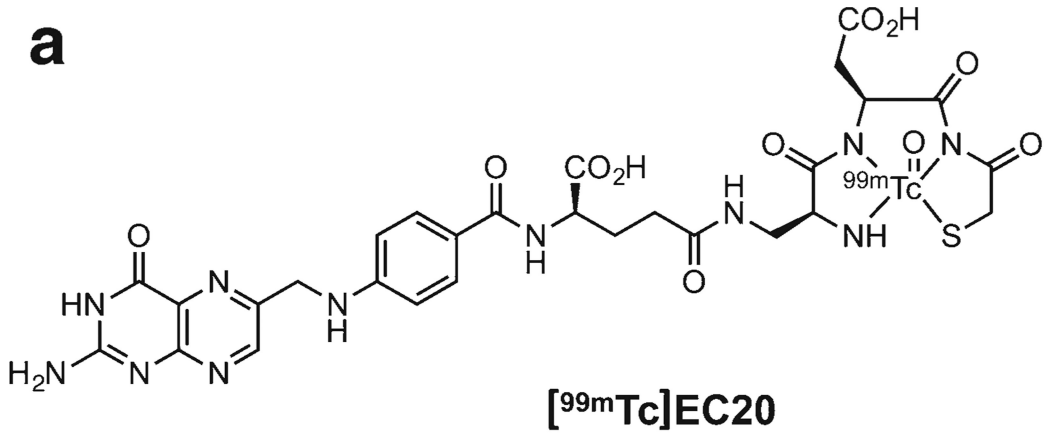

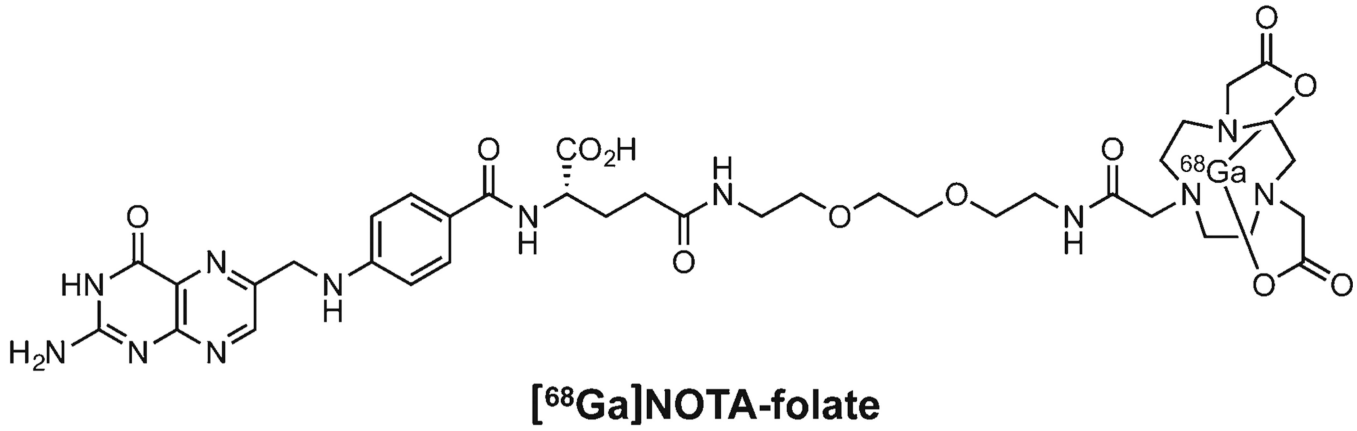

b

Compound	Radioisotope	Half-life [min]	Imaging modality
EC20	Tc-99m	364	SPECT
NOTA-folate	Ga-68	68	PET

Fig. 1.

Structures of **a** [^{99m}Tc]EC20 and [^{68}Ga]NOTA-folate, along with **b** some selected characteristics of the radiolabeled imaging tracers.

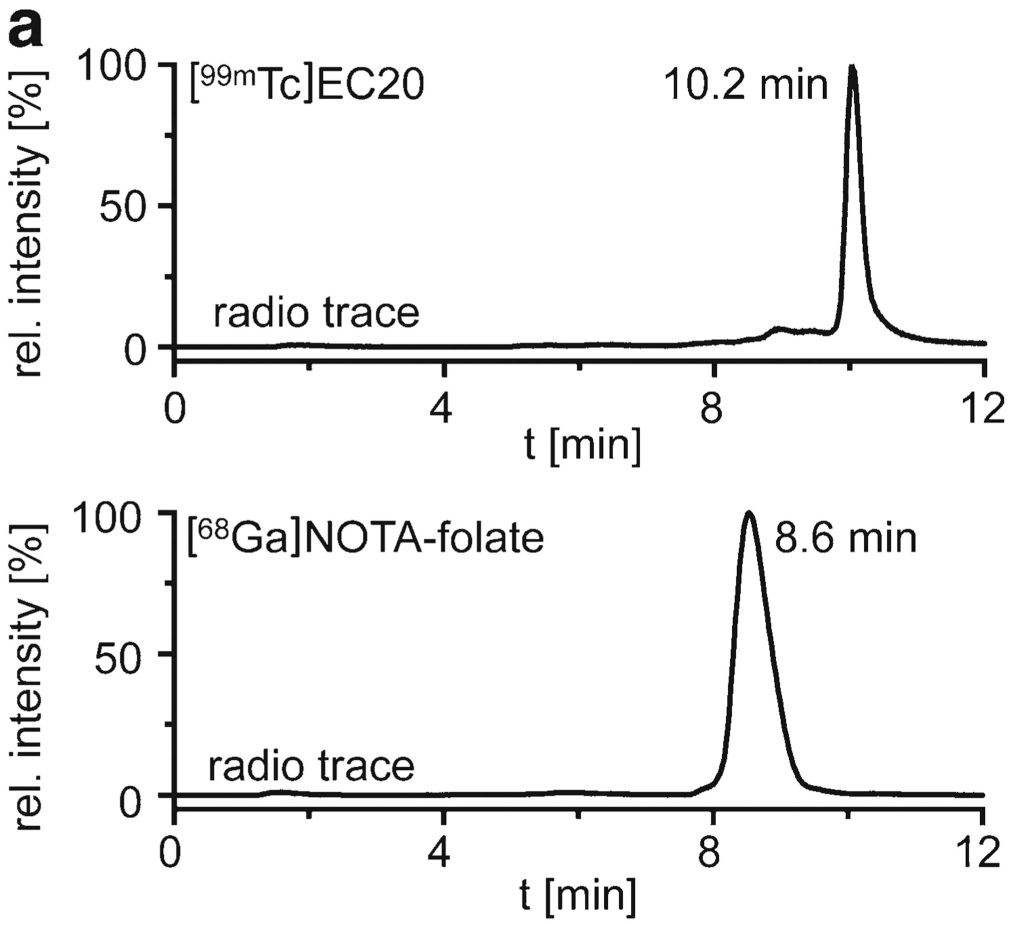

b

	RCY [%]	purity [%]	specific activity [Ci/μmol]
[^{99m}Tc]EC20	82.0 ± 2.9	91.8 ± 2.0	0.38 ± 0.02
[^{68}Ga]NOTA-folate	87.2 ± 6.9	95.6 ± 1.8	0.27 ± 0.06

Fig. 2.

Radiolabeling of PET imaging agent [^{68}Ga]NOTA-folate and SPECT imaging agent [^{99m}Tc]EC20. **a** HPLC radio chromatograms of [^{99m}Tc]EC20 (*top*) and [^{68}Ga]NOTA-folate (*bottom*) after Sep-Pak C-18 purification. **b** Decay-corrected radiochemical yield (RCY), radiochemical purity, and specific activity for [^{99m}Tc]EC20 (n = 3) and [^{68}Ga]NOTA-folate (n = 5) labeling reactions.

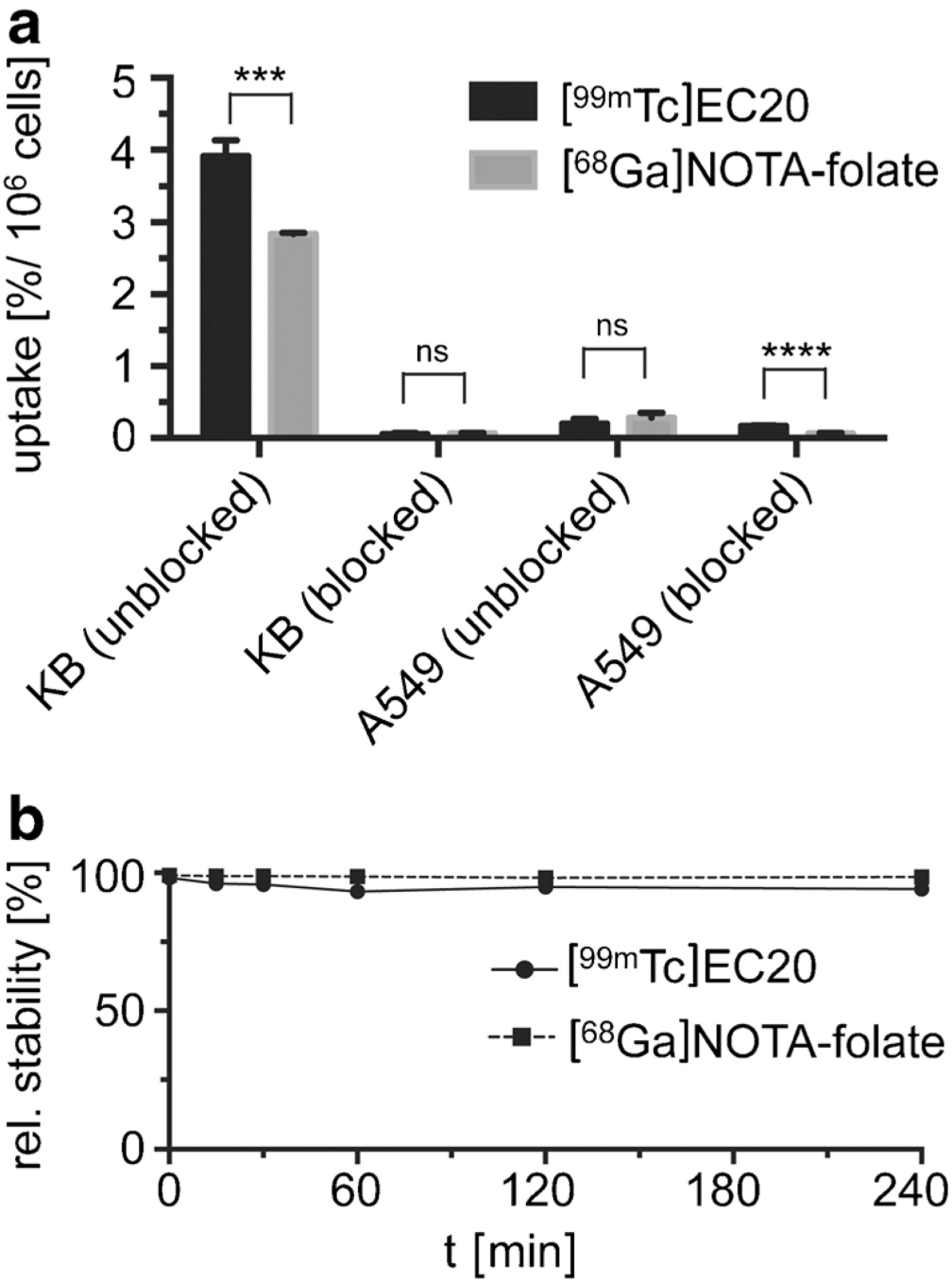

Fig. 3.

In vitro uptake and stability of [^{68}Ga]NOTA-folate. **a** *In vitro* cell uptake and retention by KB and A549 cells of either [^{68}Ga]NOTA-folate and [^{99m}Tc]EC20 (100 nM) alone or a mixture of [^{68}Ga]NOTA-folate and [^{99m}Tc]EC20 (100 nM) and folic acid (10 μM) after incubation over 30 min at 37 °C, calculated as a percentage of total added radioactivity. *P* values were calculated with Student's *t* tests, unpaired; **P* < 0.05; ***P* < 0.01; ****P* < 0.001; *****P* < 0.0001. **b** Stability studies of [^{99m}Tc]EC20 as well as [^{68}Ga]NOTA-folate in human plasma.

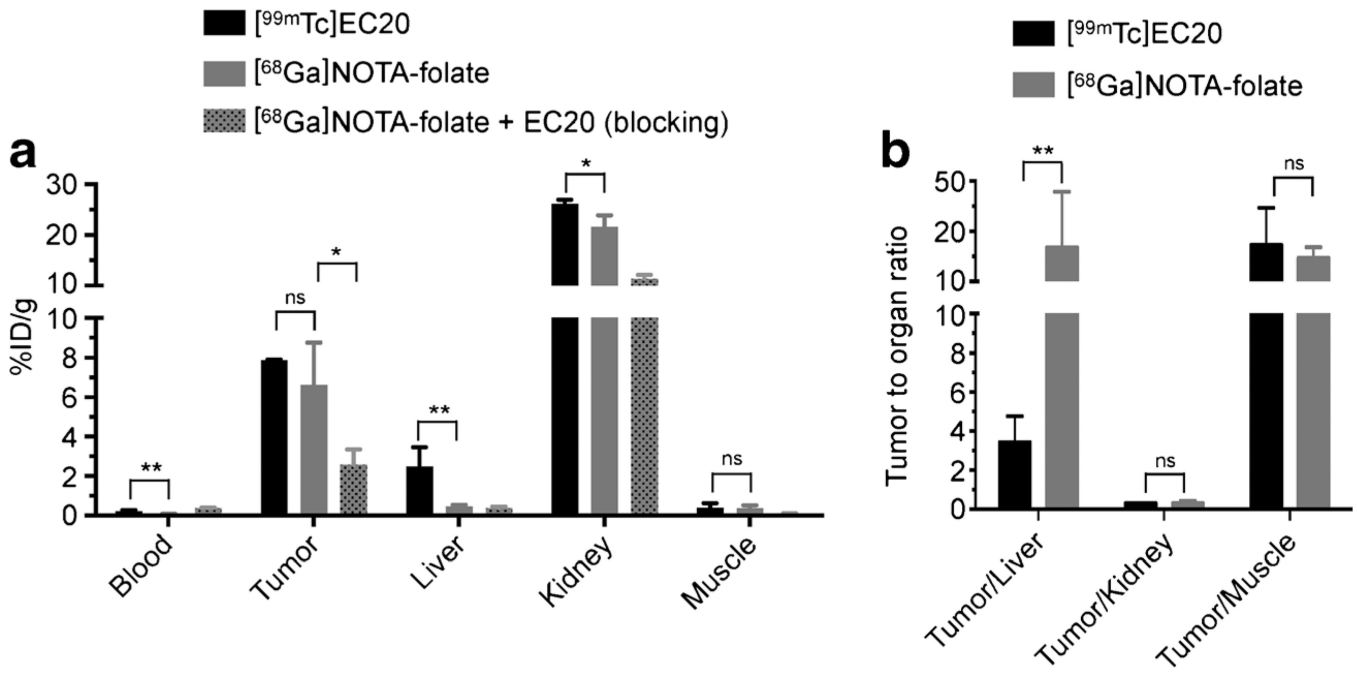

Fig. 4.

[^{68}Ga]NOTA-folate biodistribution. **a** Biodistribution data (%ID/g ± SD) of KB tumor bearing nude mice (n = 3) after 4.5 h post injection of [^{99m}Tc]EC20 (501 ± 11 μCi, 18.5 ± 0.4 MBq, 3.1 nmol, 200 μl PBS containing 10 % ethanol); [^{68}Ga]NOTA-folate (383 ± 53 μCi, 14.2 ± 2.0 MBq, 3.1 nmol, 200 μl PBS containing 10 % ethanol); or [^{68}Ga]NOTA-folate (222 ± 25 μCi, 8.2 ± 0.9 MBq, 3.1 nmol, 200 μl PBS containing 10 % ethanol) co-injected with EC20 (12.5 nmol), along with **b** selected tumor to organ ratios. Full biodistribution data is available in the supplementary materials. P values were calculated with Student's t tests, unpaired; *P < 0.05; **P < 0.01; ***P < 0.001; ****P < 0.0001.

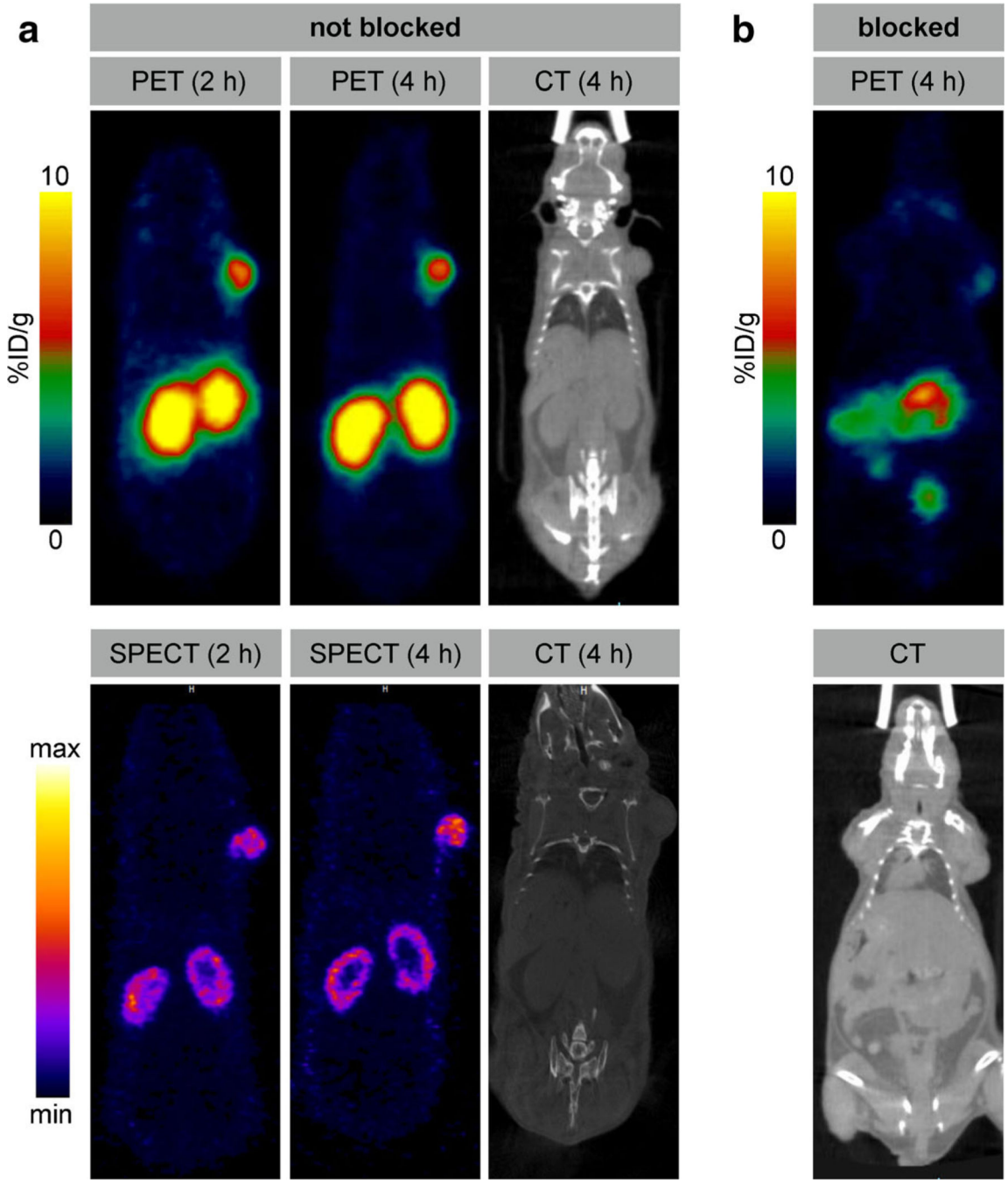

Fig. 5.

Small animal PET and SPECT imaging of KB tumor bearing mice at 2 and 4 h p.i. **a** Head-to-head comparison between [^{68}Ga]NOTA-folate (388 μCi, 14.4 MBq, 3.1 nmol, 200 μl PBS containing 10 % ethanol) and [^{99m}Tc]EC20 (511 μCi, 18.9 MBq, 3.1 nmol, 200 μl PBS containing 10 % ethanol) in the same KB tumor-bearing mice; SPECT imaging was performed 24 h post PET. **b** Blocking studies were performed by administration of

[^{68}Ga]NOTA-folate (252 μCi, 9.3 MBq, 3.1 nmol, 200 μl PBS containing 10 % ethanol) and co-injection of EC20 (12.5 nmol)